Test particle simulations of SEPs originating from an expanding shock-like source

A. Hutchinson [1]; S. Dalla [1]; T. Laitinen [1]; C. O. G. Waterfall [1]

[1] Jeremiah Horrocks Institute, University of Central Lancashire, Preston, PR1 2HE, UK

1. Introduction

We consider a 3D test particle code previously used to study solar energetic particle transport under the assumption of instantaneous injection, uniform in longitude and the sine of latitude (i.e. uniform on a spherical surface) close to the Sun (e.g. Dalla et. al. 2020; Battarbee et. al. 2018; Marsh et. al. 2013).

In this work we have developed a radially extended injection that is non-uniform in longitude and latitude that approximates particle injection from a CME-driven shock source. We present preliminary results where we consider the effects of the extended injection on intensity and anisotropy profiles of particles at 0.3 and 1.0 au. By considering the observable parameters close to the Sun (0.3 au) we aim to support observations from new spacecraft such as Solar Orbiter and Parker Solar Probe.

2. Properties of Injection Population

We consider the injection of a monoenergetic population of 100 MeV protons in a unipolar Parker spiral magnetic field (positive polarity). Our simulations include pitch angle scattering characterised by a mean free path of 0.1 au.

Instantaneous Injection

- Fixed radial distance (2.0 R$_\odot$)
- Uniform across longitudes and the sine of latitudes (i.e. uniform on a spherical surface)

Extended Injection

We consider a moving shock-like injection region that::

- Is a 50°x 50° segment of a sphere in longitude and latitude
- Injects protons between 1.2 and 100 R$_\odot$ with peak injection occurring at 5 R$_\odot$, displayed in Figure 1.
- Has an initial radial shock speed of 1500 km/s at 1.2 R$_\odot$ and is subject to constant deceleration according a relation obtained by Gopalswamy et. al. (2001).

Radial distribution

Figure 1 displays the radial distribution of particle injection described (the number of injected particles vs r) by the following equation:

$$N(r_i) = \frac{A}{(r_i - r_{ini})^B} \exp\left(\frac{-C}{r_i - r_{ini}}\right)$$

where A, B and C are positive constants, r_i is the radial position of particle injection and r_{ini} is the initial position of particle injection (1.2 R$_\odot$).

Longitudinal and Latitudinal distribution

Figure 2 displays the longitudinal and latitudinal distributions for standard deviations (σ) of 10 degrees.

- Gaussian centred on shock nose (0°, 15°).
- Different σs approximate different longitudinal dependences of particle acceleration across the shock front.

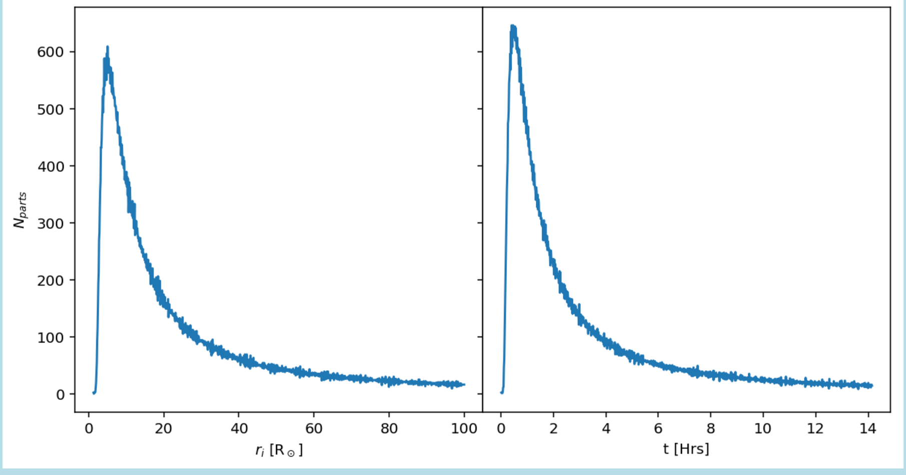

Figure 1: An example of the radial (left) and temporal (right) distributions of particle injection used in the test-particle simulations that considers a 1500km/s shock at 1.2 R$_\odot$.

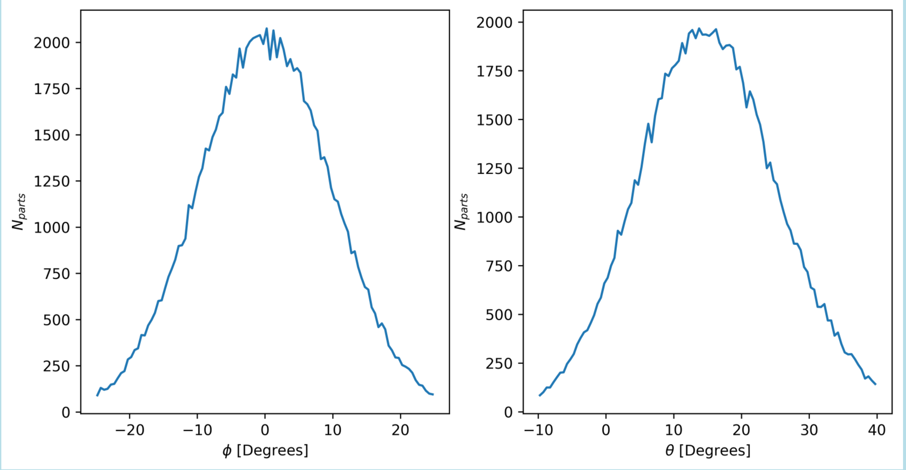

Figure 2: The longitudinal (left) and latitudinal (right) injection distributions, centred on the shock nose at (0°, 15°). Both longitudinal and latitudinal distributions here have σs of 10 degrees.

3. Instantaneous vs Extended Injection

We compare the intensity and anisotropy profiles at 1 au from an instantaneous injection and an injection extended over large radial distances in Figure 3.

Extending the injection results in:

- Higher intensities at the later times due to injection over longer times.
- Slightly lower anisotropies at the initial time due to protons injected later not having focussed as much as earlier injected particles.

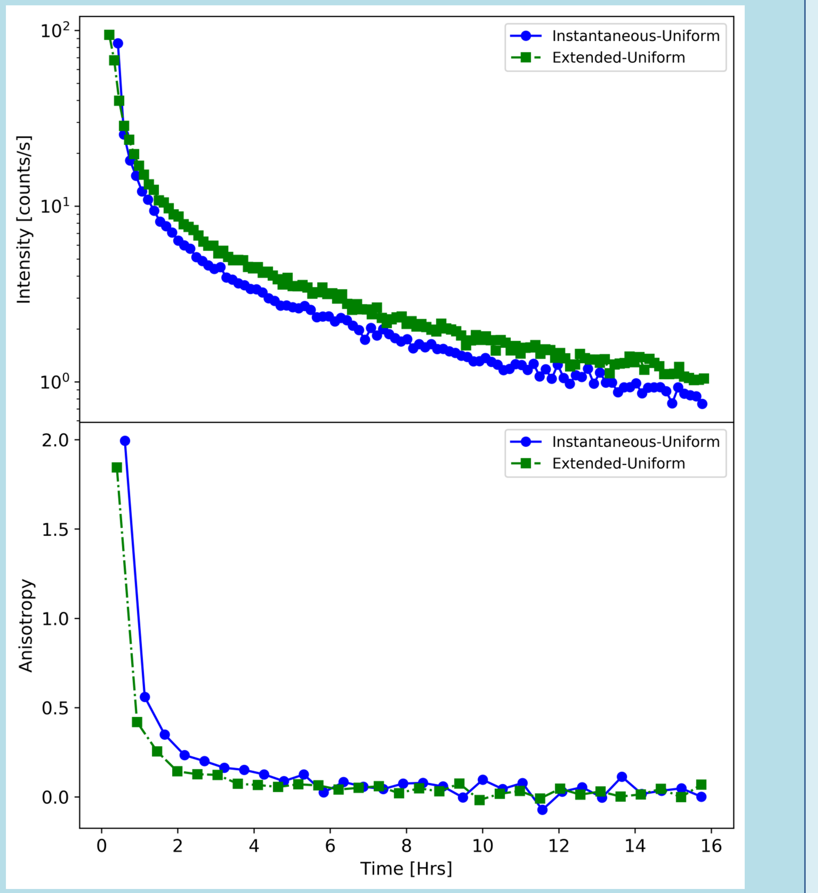

Figure 3: The intensity (top) and the anisotropy (bottom) profiles at 1 au for a 50x50 degree observation tile centred at the initial magnetically well-connected region for the first 16 hours of simulations with an instantaneous injection at 2.0 R$_\odot$ (blue circles) and a radially extended injection from 1.2 – 100 R$_\odot$ (green squares). Both injections spanned 50 degrees in longitude and latitude.

4. Uniform vs Gaussian Angular Distributions

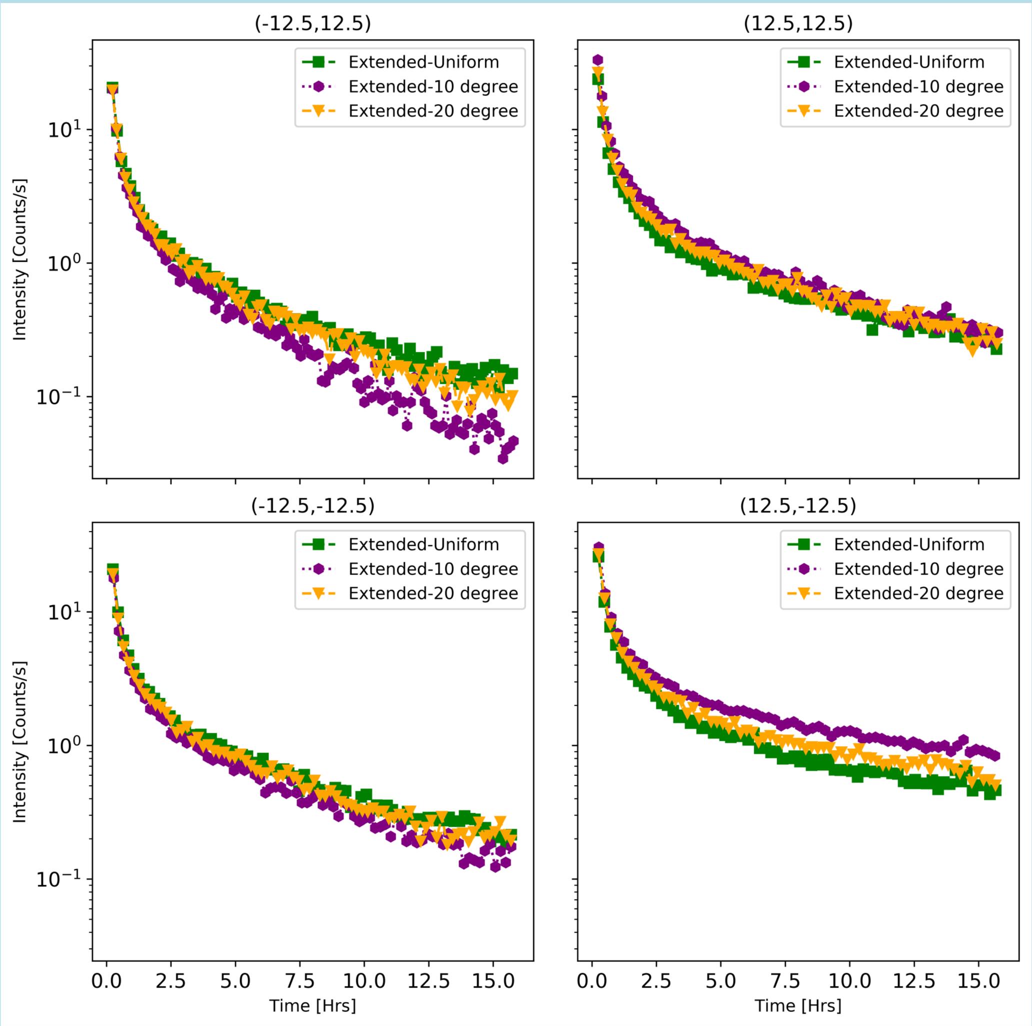

Figure 4: The intensity profiles at 1 au for the first 16 hours of simulations with the three extended injections for 25x25 degree collecting tiles located at different positions relative to the initial magnetically well-connected position (0°,0°) given by the titles of each panel. Green squares represent a uniform distribution in longitude and latitude, purple hexagons represent a gaussian injection with a standard deviation of 10 degree and yellow triangles represent a gaussian injection with a standard deviation of 20 degrees.

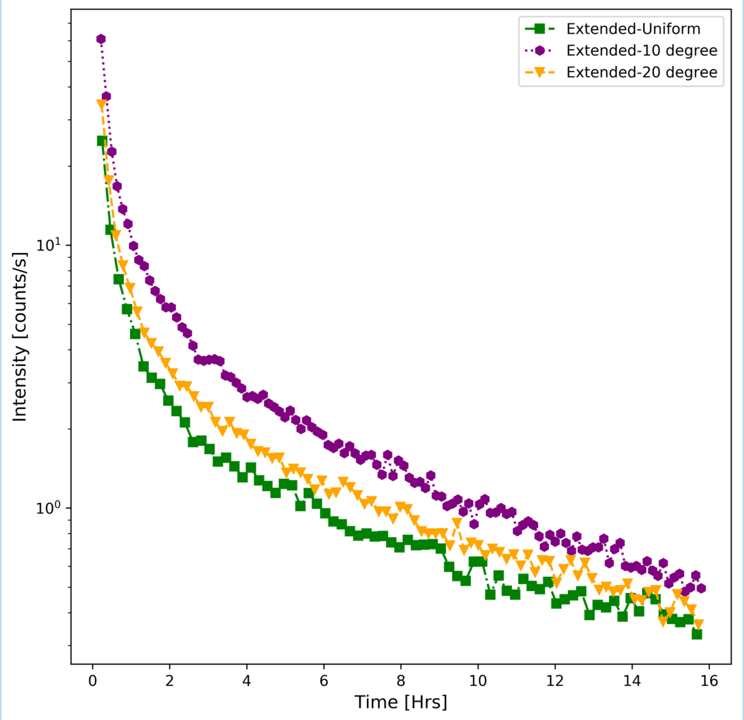

Figure 5: The intensity profiles at 1 au for the first 16 hours of simulations for the three extended injections with a 25x25 degree collecting tile located at the initial magnetically well-connected position (0° , 0°). Green squares represent a uniform distribution in longitude and latitude, purple hexagons represent a gaussian injection with a standard deviation of 10 degree and yellow triangles represent a gaussian injection with a standard deviation of 20 degrees.

- Figure 4 shows significant longitudinal dependence, with higher intensities recorded westwards of the shock nose (right panels), especially for the more shock-nose skewed injections. Faster decay phases in intensity eastwards could result from rapidly decreasing magnetic connectivity as the shock propagates radially.
- Intensities remain large southwards of the initial well-connected region due to guiding centre drifts associated with gradient and curvature of the Parker spiral (Dalla et al 2013).
- As expected, the intensities are larger for the most shock-nose skewed injection at the initial magnetically well-connected position to the shock nose, as can be seen from Figure 5.

5. Protons at 0.3 au vs 1.0 au

Figure 6 displays the intensity profiles for all four injections considered so far.

Comparing the intensity profiles at 0.3 and 1 au we find that:

- The 0.3 au profiles have higher peak intensities and faster decay phases compared to the 1 au profiles, as expected.
- The 0.3 au profiles for the extended injections have no discernible difference in the rise or decay phases.
- The rise phases at 0.3 au appear non-linear, whereas in the 1 au profiles the rise phase is linear. This is likely the result of propagation effects such as pitch angle scattering.
- All profiles for the extended injections peak at the same times. This is likely due to the common peak injection radius of 5 R$_\odot$ for each injection.

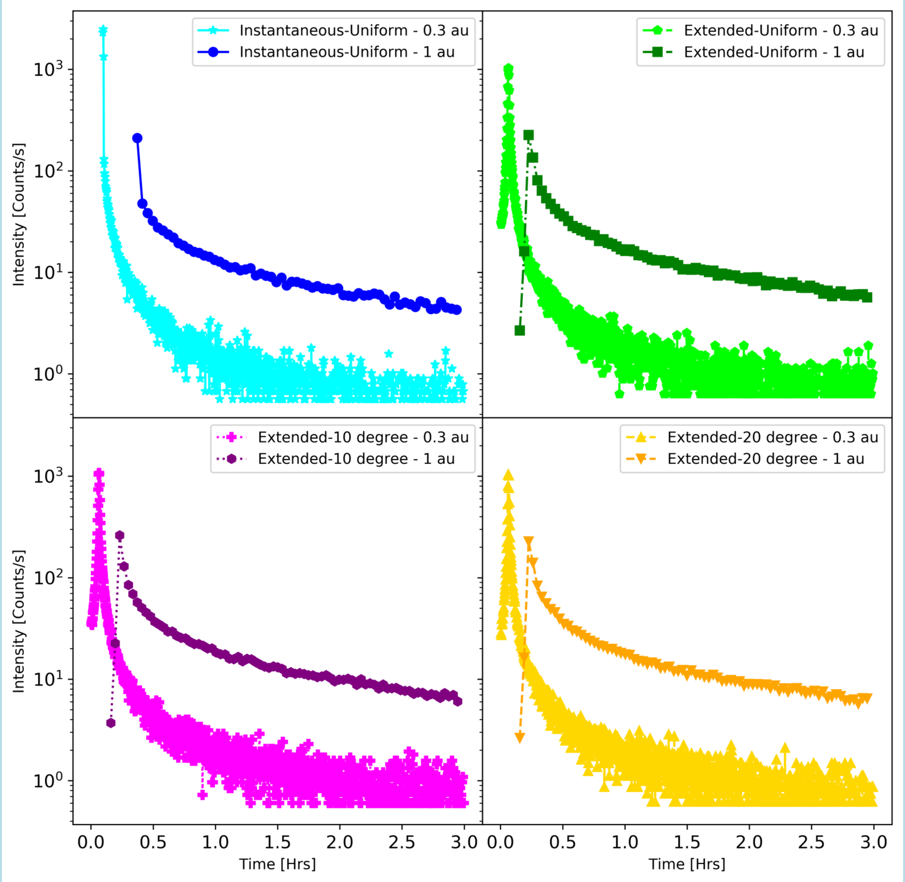

Figure 6: Intensity-time profiles for the first 3 hours of simulations with the four different injection scenarios at 0.3 au and 1.0 au, each considering a 50x50 degree collecting tile located at the initial magnetically well connected region (0°,0°) .

6. Conclusions

We studied the effects of considering extended injections in time of 100 MeV protons on their 0.3 and 1 AU intensity profiles and anisotropies. We also analysed the influence on the observables of different efficiencies of injection across the shock front.

Compared to the case of an instantaneous injection, an extended particle injection causes slower decay phases in intensity profiles and slightly lower peak anisotropies.

When considering injection efficiencies of different standard deviations (σ) across the shock, we found that a more shock-nose skewed injection results in larger intensities and slower decays measured at the initial magnetically well-connected regions at 1 au. However, faster decays are observed eastwards of the initial magnetically well-connected position as fewer protons are injected into the flux tube due to the radial motion of the particle-injecting shock.

The intensity profiles obtained at 0.3 au behave similarly for all extended injections, implying little dependence on how the particle acceleration efficiency changes in longitude and latitude across the shock front

Further Work

In upcoming work we will consider lower energy protons (10, 60 MeV) with different radial injection distributions and different peak injection positions. We also aim to consider the Heliospheric current sheet and different scattering conditions.

Acknowledgments

AH, SD, TL and COGW acknowledge support from the UK Science and Technology Facilities Council (STFC), through a Doctoral Training grant - ST/T506011/1 and grant ST/R000425/1.

Contact

Adam Hutchinson

Jeremiah Horrocks Institute, University of Central Lancashire

Email: ahutchinson3@uclan.ac.uk

References

- Battarbee, M., Dalla, S., & Marsh, M.S. (2018), ApJ, 854:23 (14pp), doi: 10.3847/1538-4357/aaafa
- Dalla, S., Marsh, M. S. , Kelly, J., Laitinen, T. (2013), *JGR Space Physics*, *118*, 5979–5985, doi:10.1002/jgra.50589
- Dalla, S., de Nolfo, G. A., Bruno, A., Giacalone, J., Laitinen, T., Thomas, S., Battarbee, M., & Marsh, M.S., (2020), A&A, 639, A105, doi: 10.1051/0004-6361/201937338
- Gopalswamy, N., Lara, A., Yashiro, S., Kaiser, M. L., & Howard, R. A.2001, *JGR Space Physics*, 106, 29207,doi: 10.1029/2001JA00017710.1029/2001JA000177
- Marsh, M. S., Dalla, S., Kelly, J., & Laitinen, T., (2013), ApJ, 774:4, (9pp), doi:10.1088/0004-637X/774/1/4

ONLINE ICRC 2021 THE ASTROPARTICLE PHYSICS CONFERENCE Berlin | Germany
37th International Cosmic Ray Conference 12–23 July 2021